Electron-electron scattering in narrow Si accumulation layers

1989 J. Phys.: Condens. Matter 1 3289

(http://iopscience.iop.org/0953-8984/1/20/010)

J. Phys.: Condens. Matter **1** (1989) 3289–3293. Printed in the UK

LETTER TO THE EDITOR

Electron–electron scattering in narrow Si accumulation layers

D M Pooke†‡, N Paquin†§, M Pepper† and A Gundlach‖
† Cavendish Laboratory, Madingley Road, Cambridge CB3 0HE, UK
‖ Edinburgh Microfabrication Facility, King's Building, Edinburgh EM9 3JL, UK

Received 10 February 1989

Abstract. We report on measurements of the phase coherence time, τ_φ, as determined from the measurement of weak negative magnetoresistance in narrow pinched Si accumulation layers. Under favourable bias conditions, one-dimensional quantum interference and electron interaction corrections to the conductivity are found. The phase coherence length is then best described in terms of the 1D Nyquist phase-breaking mechanism, with a Landau–Baber (pure metal limit) component which retains its 2D form.

There is substantial interest in the nature of quantum transport in disordered systems of low dimensions, encouraged in part by improved techniques for fabricating the fine scale structures. Recent experimental work includes studies on fine wires [1, 2], narrow metal films [3], narrow Si metal–oxide–semiconductor field-effect transistors (MOSFETs) [4–6] and GaAs/AlGaAs heterostructures [7, 8]. In this Letter we report on measurements of the quantum interference (weak localisation) correction to the conductivity, extending to the quasi-one-dimensional regime, in narrow Si pinched accumulation layer MOSFETs.

The dimensionality of a sample with respect to the quantum interference effect is governed by the magnitude of the phase coherence length, L_φ, relative to the sample dimensions. For the Si MOSFET the correction will take its one dimensional form if $L_\varphi > W$, where W is the channel width (with it assumed that the channel length, L, satisfies $L \gg L_\varphi$). Application of a magnetic field B transverse to the plane of the channel quenches the quantum interference giving a weak positive magnetoconductance; in one dimension (1D) the theoretical relation is [9]

$$\Delta g(B) = (e^2/\pi\hbar L)\{L_\varphi - [(1/L_\varphi^2) + (e^2W^2B^2/3\hbar^2)]^{-1/2}\}. \tag{1}$$

This assumes negligible boundary scattering ($W \gg l$, where l is the elastic scattering length), and is valid only for $L_H > W$, where L_H is the magnetic length defined by $L_H = (\hbar/2eB)^{1/2}$. Significant decrease of L_φ or L_H below W results in 2D behaviour for which the theoretical relations are well established [10].

Contributions to the magnetoconductance arising from the electron interaction correction are expected to be negligible in the weak localisation regime [11], hence the value of L_φ may be obtained by fitting the theoretical relation (1) to the experimentally

‡ Present address: Physics and Engineering Laboratory, DSIR, PO Box 31313, Lower Hutt, New Zealand
§ Present address: MPB Technology Inc, Dorval, Quebec, Canada H9P 1J1

0953-8984/89/203289 + 05 $02.50

observed low field magnetoconductance. L_φ is related to the phase coherence time τ_φ through the relation $L_\varphi = (D\tau_\varphi)^{1/2}$ where D is the diffusion constant.

At low temperatures the dominant phase breaking mechanism is electron–electron scattering; this has been the subject of much theoretical and experimental study [11]. In the pure metal limit (no disorder) the electron–electron scattering time τ_{ee} is described by the Landau–Baber result and in 2D is given by [12]

$$(\tau^0_{ee})^{-1} = (1/n_v)(\pi/2)F^2(k^2T^2/\hbar E_F)\ln(1/\delta) \tag{2}$$

where δ is the cut-off parameter, $\max[\hbar/\tau E_F, kT/E_F]$, E_F is the Fermi energy and F is the screening factor. The dimensionality here relates to that of the effective density of states; for a 1D density of states (DOS) the term is linear in T.

In the presence of disorder the scattering rate is enhanced, with a contribution $(\tau^i_{ee})^{-1}$ having a temperature dependence going as [12] $T^{d/4}$ and hence which dominates $(\tau^0_{ee})^{-1}$ as $T \to 0$. The dimensionality d of this term is determined by the thermal length L_T in the same manner that L_φ determines that of the quantum interference correction. The total scattering rate is the sum of two components, $(\tau_{ee})^{-1} = (\tau^0_{ee})^{-1} + (\tau^i_{ee})^{-1}$, L_T is given by $(\hbar D/kT)^{1/2}$.

In the current understanding of the phase breaking mechanism [13, 14] it is stressed that the τ_φ appearing in the weak localisation correction is not, in fact, the lifetime τ_{ee}, but rather the lifetime of the two-particle correlation function which describes quantum interference. τ_φ and τ_{ee} coincide where electron collisions involving large energy transfer dominate the phase breaking process, but for $d \leqslant 2$ an important contribution comes from small energy transfer (quasi-elastic) processes equivalent to a Nyquist rate [13, 15], $(\tau_N)^{-1}$. In the regime $kT\tau_\varphi \geqslant \hbar$, $(\tau_N)^{-1}$ is expected to dominate $(\tau^i_{ee})^{-1}$ so that $\tau_\varphi \equiv \tau_N$.

In 2D $(\tau_N)^{-1}$, like $(\tau^i_{ee})^{-1}$, is linear in T. In 1D, though, $(\tau_N)^{-1} \simeq T^{-2/3}$, while $(\tau^i_{ee})^{-1} \simeq T^{-1/2}$. Specifically, in 1D τ_N is given by the theoretical relation [13]

$$(\tau_N)^{-1} = ((2D)^{1/2}e^2kT/gL\hbar^2)^{2/3}. \tag{3}$$

In 1D, then, the different phase-breaking mechanisms may be distinguished by examining the temperature dependence of the τ_φ extracted from magnetoresistance experiments.

The devices used in the experiments are polysilicon-gated, pinched accumulation layer Si(100) MOSFETs which have been described elsewhere [16]. The application of a reverse voltage bias, V_p, to p+ implants along the 100 μm length of channel reduces the width of the electron layer. The width under various gate (V_g) and p+ biases can be determined from magnetoresistance measurements in the 2D regime [17]; these are listed in table 1 with other transport parameters.

Table 1. Relevant transport parameters at various gate, V_g, and control junction, V_p, biases.

V_g (V)	60	60	75
V_p (V)	0	−3	−6
$g_B(10^{-6}\,\Omega^{-1})$	8.2	4.6	3.6
$D(10^{-3}\,m^2\,s^{-1})$	7.2	6.7	7.1
$n(10^{16}\,m^{-2})$	2.1	1.85	2.1
$k_F l$	24	22	23
$\mu(m^2\,V^{-1}\,s^{-1})$	0.57	0.57	0.54
$l\,(10^{-2}\,\mu m)$	9.4	9.4	10.0
$W(\mu m)$ at $T = 4.2$ K	0.44	0.26	0.20

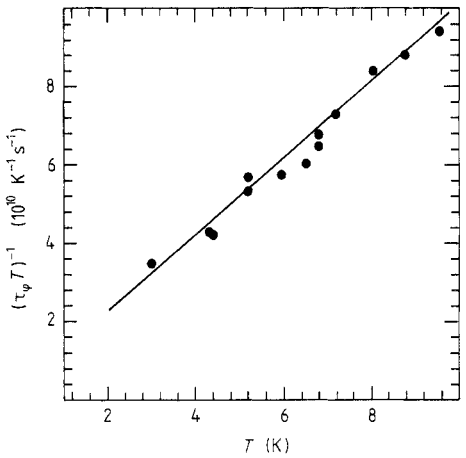

Figure 1. $(\tau_\varphi T)^{-1}$ plotted against T for the 2D regime ($V_g = 60$ V, $V_p = 0$ V). The full line is the best linear fit to the data.

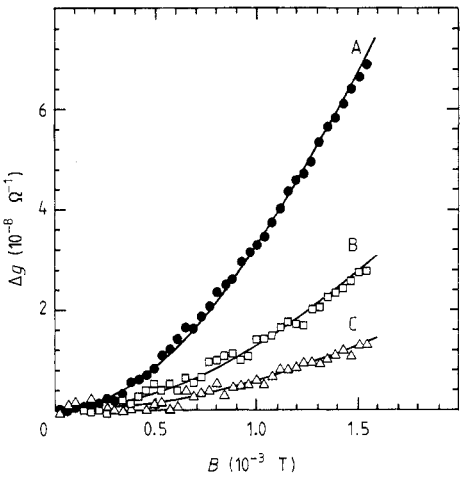

Figure 2. Weak localisation magnetoconductance at the temperatures indicated ($V_g = 60$ V, $V_p = 0$ V). The full curves are fits of the 1D magnetoconductance expression (1) to the data: *A*, $T = 0.14$ K; *B*, $T = 0.41$ K; *C*, $T = 0.72$ K.

The low temperature ($T < 1$ K) magnetoresistance measurements were collected using a computer-controlled data acquisition system, allowing data averaging to improve signal-to-noise levels. Care was taken to ensure that negligible electron heating resulted from this arrangement.

For T much beyond 1 K the device, with biases $V_g = 60$ V and $V_p = 0$ V, is in the 2D localisation regime ($L_\varphi < W$, with the magnetoresistance fitting the 2D expression [10]). Figure 1 displays the quantity $(\tau_\varphi T)^{-1}$ for $3 < T < 10$ K. The linear fit shows τ_φ is described by the relation $(\tau_\varphi)^{-1} = A(T/\mathrm{K}) + B(T/\mathrm{K})^2$, as can be expected in 2D [18]. Here $A = (3.5 \pm 3.4) \times 10^9\ \mathrm{s}^{-1}$ and $B = (9.72 \pm 0.05) \times 10^9\ \mathrm{s}^{-1}$.

At lower temperatures the device enters the 1D regime, $L_\varphi > W$. The magnetoresistance for $T < 1$ K is well fitted (figure 2) by (1), while the 2D expression could not be used with realistic parameters. The resulting values of L_φ are shown in figure 3. The best single power-law fit to the data, excluding points below 150 mK (which will be discussed later) gives $L_\varphi = (0.41 \pm 0.01)\ \mu\mathrm{m}\ (T/\mathrm{K})^{-0.39 \pm 0.03}$, in good agreement with the theoretical prediction for the 1D Nyquist mechanism of $L_N = 0.51\ \mu\mathrm{m}\ (T/\mathrm{K})^{-1/3}$.

The discrepancy in the power of temperature does however require further consideration. From the data we see that $L_T > W$ only for $T < 0.3$ K so above 0.3 K the 2D limit of electron–electron scattering could be expected, giving $L_\varphi \simeq T^{-1/2}$. This would demonstrate how a sample may be 1D with respect to quantum interference, $L_\varphi > W$, and yet with $L_T < W$ still have the magnitude and temperature dependence of L_φ governed by the 2D equations. If this were the case the temperature coefficient for the 2D term $\tau_\varphi \simeq T^{-1}$ (i.e., $L_\varphi \simeq T^{-1/2}$) should match that found for $T > 3$ K, $A = 3.5 \times 10^9\ \mathrm{s}^{-1}$ from above. In fitting L_φ to $T^{-1/2}$ for $0.4\ \mathrm{K} < T < 1$ K (as shown in figure 3) a temperature prefactor of $0.39 \pm 0.006\ \mu\mathrm{m}$ is obtained. But, using D from table 1, this equates to $(\tau_\varphi)^{-1} = (4.7 \pm 0.2) \times 10^{10}\ \mathrm{s}^{-1}$, in poor agreement with the value A. This is only marginally improved if the pure metal limit term $(L_\varphi)^{-2} \simeq T^2$, with coefficient B, is also included in fitting the $0.4 < T < 1$ K data. However for the points below 0.4 K we

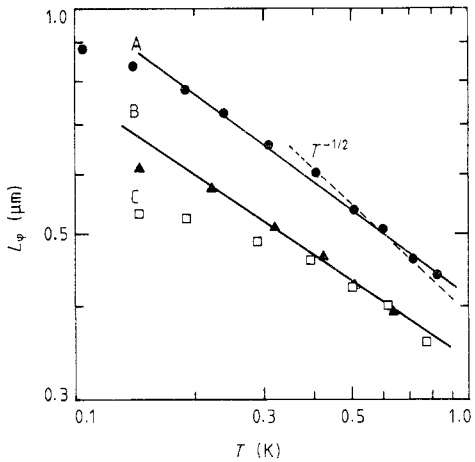

Figure 3. The T dependence of the phase-coherence length for the three sets of bias conditions; (*a*) $V_g = 60$ V, $V_p = 0$ V; (*b*) $V_g = 60$ V, $V_p = -3$ V; (*c*) $V_g = 75$ V, $V_p = -6$ V. The solid lines are the best fits for a single power of temperature, excluding points below 150 mK, giving (A) $L_\varphi \simeq T^{-0.39}$ and (B) $L_\varphi \simeq T^{-0.34}$. The dashed line is the best $T^{-1/2}$ fit to the data for $T > 0.4$ K. The data for (C) falls below the $T^{-1/3}$ 1D Nyquist prediction.

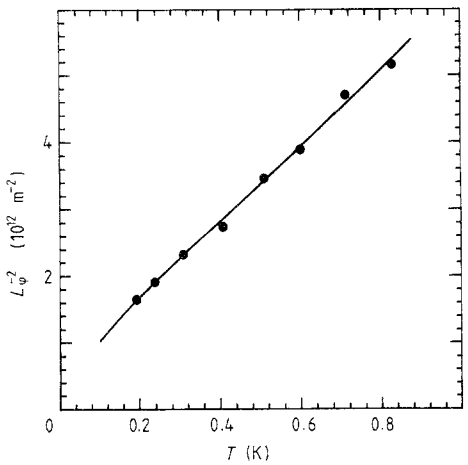

Figure 4. The inverse square of the phase coherence length plotted against temperature ($V_g = 60$ V, $V_p = 0$ V). The solid line is the best fit to a combination of T^2 and $T^{2/3}$ terms ($X T^{2/3} + Y T^2$), corresponding to contributions from both the 2D Landau–Baber and 1D Nyquist phase-breaking mechanisms.

find $L_\varphi = (0.45 \pm 0.01)\ \mu\text{m}\ (T/\text{K})^{-0.34 \pm 0.02}$ which agrees with the Nyquist prediction, though the data range is very limited.

A more satisfactory explanation for the discrepancy in the power of temperature ($T^{-0.39}$ versus $T^{-1/3}$) is that the 1D Nyquist mechanism operates throughout the temperature range to $T = 1$ K (the dimensionality condition $L_T > W$ is approximate, with $\pi L_T > W$ often being used), together with a contribution from the 2D Landau–Baber term (2D because the DOS remains two-dimensional). In this case the data should fit the form $(L_\varphi)^{-2} = X(T/\text{K})^{2/3} + Y(T/\text{K})^2$, in the same fashion as for 2D systems [18]. This fit is shown in figure 4, yielding $X = (4.7 \pm 0.1) \times 10^{12}\ \text{m}^{-2}$ or $X^{-1/2} = (0.46 \pm 0.005)\ \mu\text{m}$, in good agreement with the Nyquist prediction. In this explanation the value of (YD) should match B, the T^2 coefficient of $(\tau_\varphi)^{-1}$ from the 2D regime. From figure 4 and table 1, $YD = (1.1 \pm 0.1) \times 10^{10}\ \text{s}^{-1}$, in excellent accord with B. In addition, $\tau_N \ll \tau_{ee}^0$ which is required to allow for such a linear combination [13].

It could be argued that the data represents a linear combination of T^2 $((\tau_{ee}^0)^{-1})$ and $T^{1/2}$ $((\tau_{ee}^i)^{-1}$ in 1D) terms instead, with the Nyquist mechanism not operating at all. The T^2 coefficient should still match as before; this is not evident, with a value of 2.0×10^{10} s^{-1} being obtained in this case. Hence the most likely explanation is that $L_\varphi(T)$ is determined by the 1D Nyquist mechanism with a contribution from the 2D Landau–Baber term.

For $V_g = 60$ V, $V_p = -3$ V, L_φ and L_T are greater than W over the entire temperature range. The best power law fit, as shown in figure 3, is given by $L_\varphi = (0.34 \pm 0.01)\ \mu\text{m}\ (T/\text{K})^{-0.36 \pm 0.03}$ which compares favourably with the 1D Nyquist prediction of $0.41\ \mu\text{m}\ (T/\text{K})^{-1/3}$.

For $V_g = 75$ V, $V_p = -6$ V, the temperature dependence drops (figure 3) below $T^{-1/3}$ at a higher temperature than noted in the previous results. It is possible that the

phase-breaking mechanism is becoming dominated by the large energy-transfer mechanism τ_{ee}^{i} ($L_\varphi \simeq T^{-1/4}$ in 1D). Indeed, the values of the parameter $kT\tau_\varphi/\hbar$ at $T = 145$ mK are 1.75, 1.07 and 0.77 respectively for the three sets of bias conditions considered, indicating the Nyquist mechanism need not dominate τ_{ee}^{i} at the lowest temperatures. However, we note that additional structure in the magnetoresistance traces for $T < 150$ mK makes the analysis less reliable in this region [16].

In conclusion, we have examined the temperature dependence of the phase breaking mechanism in the quasi-1D regime by analysing the weak localisation negative magnetoresistance. In the most interesting case L_φ is best described by a combination of the 1D Nyquist mechanism with a contribution from the 2D Landau–Baber term. In a narrower channel the data is well described by the 1D Nyquist mechanism.

This work was supported by the Science and Engineering Research Council and, in part, by the European Research Office of the US Army. We thank the Edinburgh Microfabrication Facility staff for their assistance in the preparation of samples. D Pooke wishes to thank the National Research Advisory Council of New Zealand for a Postgraduate Fellowship.

References

[1] Lin J J and Giordano N 1986 *Phys. Rev.* B **33**, 1519; 1988 **35** 545
[2] Heraud A P, Beaumont S P, Wilkinson C D W, Main P C, Owens-Bradley J R and Eaves L 1987 *J. Phys. C: Solid State Phys.* **20** L249
[3] Beutler D E and Giordano N 1988 *Phys. Rev.* B **38** 8
[4] Warren A C, Antoniadis D A and Smith H I 1986 *Phys. Rev. Lett.* **56** 1858
[5] Webb R A, Fowler A B, Hartstein A and Wainer J J 1986 *Surf. Sci.* **170** 14
[6] Skocpol W J, Mankiewich P M, Howard R E, Jackel L D, Tennant D M and Stone A D 1987 *Phys. Rev. Lett.* **58** 2347
[7] Thornton T J, Pepper M, Ahmed H, Andrews D and Davies G J 1986 *Phys. Rev. Lett.* **56** 1198
[8] Choi K K, Tsui D C and Palmateer S C 1986 *Surf. Sci.* **170** 702
[9] Altshuler B L and Aronov A G 1981 *JETP Lett.* **33** 499
[10] Hikami S, Larkin A I and Nagaoka Y 1980 *Prog. Theor. Phys.* **63** 707
[11] Lee P A and Ramakrishnan T V 1985 *Rev. Mod. Phys.* **57** 289
[12] Fukuyama H and Abrahams E 1983 *Phys. Rev.* B **27** 5976
[13] Altshuler B L and Aronov A G 1985 *Electron–Electron Interactions in Disordered Systems* ed. A L Efros and M Pollak, (Amsterdam: North Holland) p 1
[14] Fukuyama H 1985 *Electron–Electron Interactions in Disordered Systems* ed. A L Efros and M Pollak (Amsterdam: North Holland) p 154
[15] Altshuler B L, Aronov A G and Khmelnitskii D E 1982 *J. Phys. C: Solid State Phys.* **15** 7367
[16] Pooke D M, Mottahedeh R, Pepper M and Gundlach A 1988 *Proc. EP2DS-VII, Surf. Sci.* **196** 59
[17] Dean C C and Pepper M 1982 *J. Phys. C: Solid State Phys.* **15** L1287
[18] Davies R A and Pepper M 1983 *J. Phys. C: Solid State Phys.* **16** L353